Supporting Information

Chemical and Photochemical Water Oxidation Catalyzed by Novel Ruthenium Complexes Comprising a Negatively Charged NC^{NHC}O Ligand

Wei Su,[a] Hussein A. Younus,[a] Kui Zhou,[a] Zafar A. K. Khattak,[a] Somboon Chaemcheun,[a] Cheng Chen[a,*] and Francis Verpoort[a,b,c,*]

[a.] *State Key Laboratory of Advanced Technology for Materials Synthesis and Processing, Wuhan University of Technology, Wuhan, PR China.*

[b.] *National Research Tomsk Polytechnic University, Lenin Avenue 30, 634050 Tomsk, Russian Federation.*

[c.] *Ghent University, Global Campus Songdo, 119 Songdo, munhwa-Ro, Ywonsu-Gu, Incheon, Republic of Korea.*

E-mails: francis.verpoort@ugent.be

Synthetic procedure of ligand 1

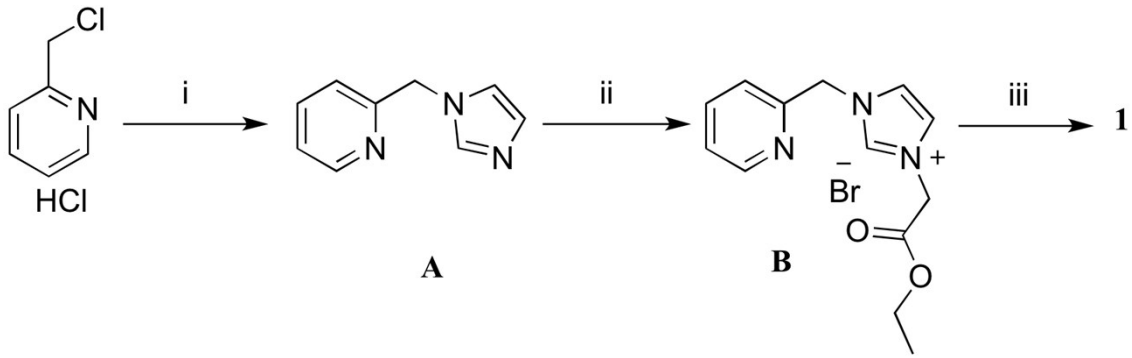

Scheme S1. Synthetic procedure to carbene precursor **1**. i) 1H-imidazole, KOH, THF, reflux, 12 h; ii) Ethyl Bromoacetate, anhydrous THF, reflux, 12 h; iii) KOH, H_2O/iPrOH=1/3, reflux, 5 h.

Synthesis of A

Potassium hydroxide (40 mmol, 2.4 g) was added into a 250 ml round bottom flask containing a solution of 1H-imidazole (20 mmol, 1.4 g) in THF. The mixture was refluxed for 2 hours, resulting in the formation of potassium imidazolide. Subsequently, 2-chloromethyl pyridine hydrochloride (20 mmol, 3.2 g) was added and refluxed overnight. After cooling to room temperature, violates was removed using a rotavapor. The residue was dissolved in water and extracted with dichloromethane. The organic layer was dried using anhydrous sodium sulfate, concentrated and purified via flash chromatography (methanol/DCM=1/15) to give a brown solid. Yield: 66 %, 2.1 g. The spectra data is consistent with reported literature[S1]. ^{1}H NMR (500 MHz, $CDCl_3$, 25 ℃) δ= 8.58 (s, 1H, NCH_{arom}), 7.66 (t, J = 7.6 Hz, 1H, CH_{arom}), 7.61 (s, 1H, CH_{arom}), 7.23 (s, 1H, CH_{arom}), 7.10 (s, 1H,

CH_{imi}), 6.99 (s, 1H, CH_{imi}), 6.95 (d, J = 7.7 Hz, 1H, CH_{arom}), 5.24 (s, 2H, -CCH_2N-). ^{13}C NMR (125 MHz, $CDCl_3$, 25℃) δ= 206.97, 156.11, 149.66, 137.62, 137.31, 129.83, 123.02, 121.18, 119.49, 52.48,

Synthesis of B

A mixture of **A** (8.8 mmol, 1.4 g) and ethyl bromoacetate (8.8 mmol, 1.5 g) in dry THF was heated at 70 °C overnight to give an off-white precipitate. The solid was collected, washed 3 times with THF and dried under vacuum. Yield: 2.4 g, 83 %. ^1H NMR (500 MHz, [d6]DMSO, 25 ℃) δ= 9.30 (s, 1H, $NCH_{imi}N$), 8.56 (d, J = 4.5 Hz, 1H, NCH_{arom}), 7.90 (td, J = 7.7, 1.7 Hz, 1H, CH_{arom}), 7.83 (s, 1H, CH_{imi}), 7.78 (s, 1H, CH_{imi}), 7.50 (d, J = 7.8 Hz, 1H, CH_{arom}), 7.42 (dd, J = 7.3, 5.0 Hz, 1H, CH_{arom}), 5.65 (s, 2H, -NCH_2C=O), 5.29 (s, 2H, -CCH_2N-), 4.22 (q, J = 7.1 Hz, 2H, -CH_2CH_3), 1.24 (t, J = 7.1 Hz, 3H, -CH_3). ^{13}C NMR (125 MHz, [d_6]DMSO, 25 ℃) δ= 167.27, 153.87, 150.12, 138.46, 138.07, 124.34, 124.23, 123.44, 123.05, 62.39, 53.63, 50.11, 14.37.

Synthesis of 1

A solution containing **B** (1 g, 3.07 mmol) and potassium hydroxide in H_2O/iPrOH (3/1) was refluxed for 5 h. After cooling to room temperature, the volatile was evaporated under vacuum. The residue was redissolved in methanol and filtered. The filtrate was dried. Subsequent recrystallization with MeOH/ethyl acetate afforded 1 as a white powder. Yield: 660 mg, 99%. ^1H NMR (500 MHz, [d_6]DMSO, 25 ℃) :δ=9.18 (s, 1H, $NCH_{imi}N$), 8.56 (d, J = 4.7 Hz, 1H, $CCH_{arom}N$), 7.88 (td, J = 7.7, 1.8 Hz, 1H, CH_{arom}), 7.66 (s, 1H, CH_{imi}), 7.61 (s, 1H, CH_{imi}), 7.46 (d, J = 7.8 Hz, 1H, CH_{arom}), 7.40 (dd, J = 6.8, 4.9 Hz, 1H, CH_{arom}), 5.56 (s, 2H, NCH_2N), 4.46 (s, 2H, NCH_2C). ^{13}C NMR (125 MHz, [d_6]DMSO, 25 ℃): δ=166.29, 154.34, 150.0, 138.02, 137.58, 124.14, 122.90, 122.11, 53.44, 53.36.

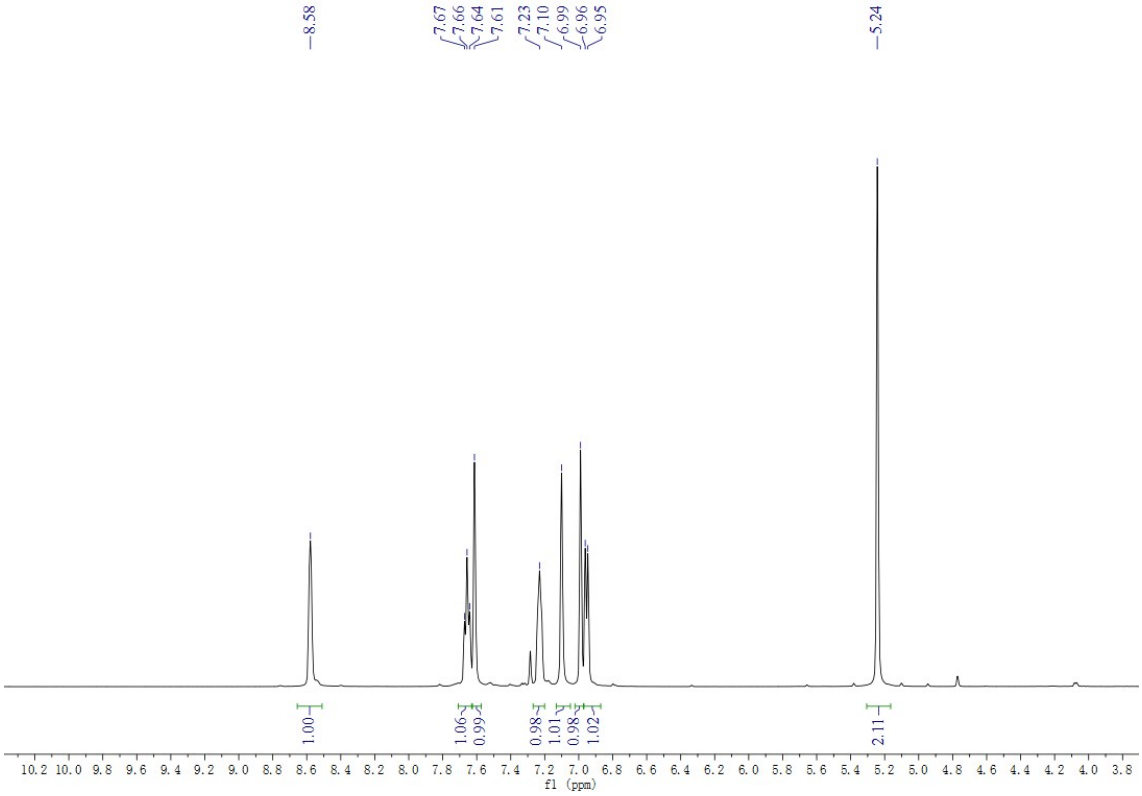

Figure S1. ^{1}H-NMR spectrum of compound **A** in $CDCl_3$.

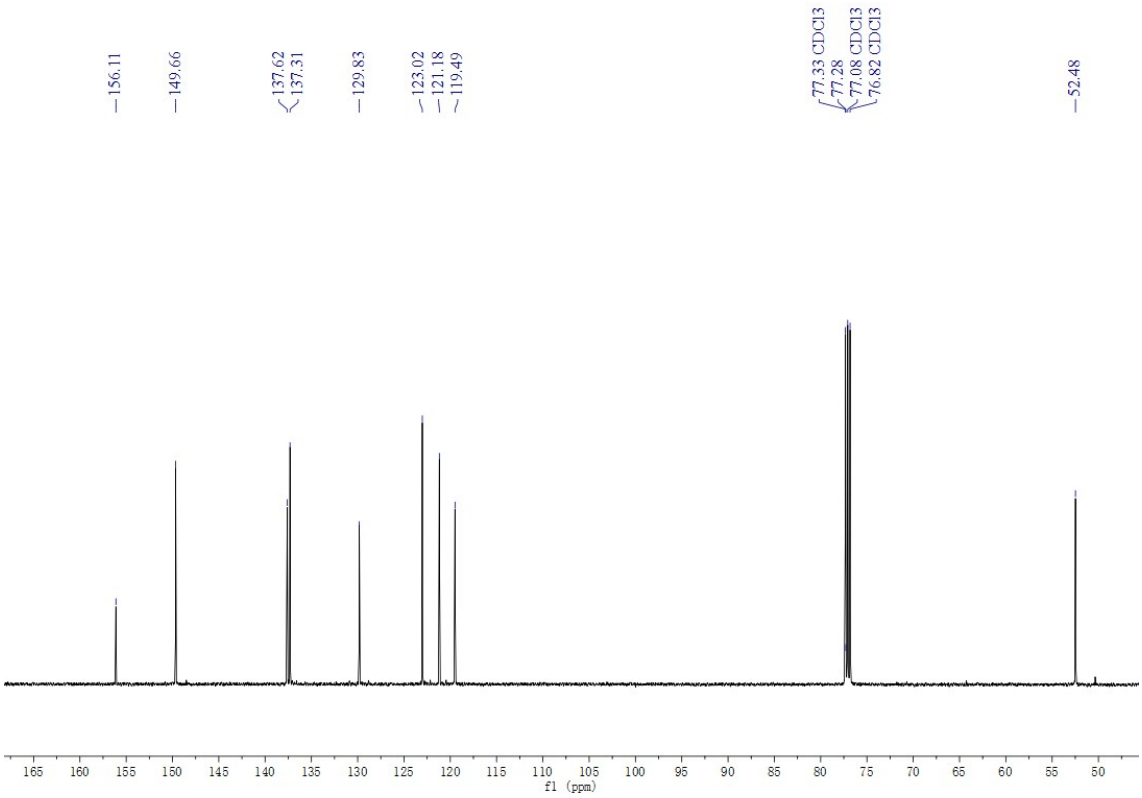

Figure S2. ^{13}C-NMR spectrum of compound **A** in $CDCl_3$.

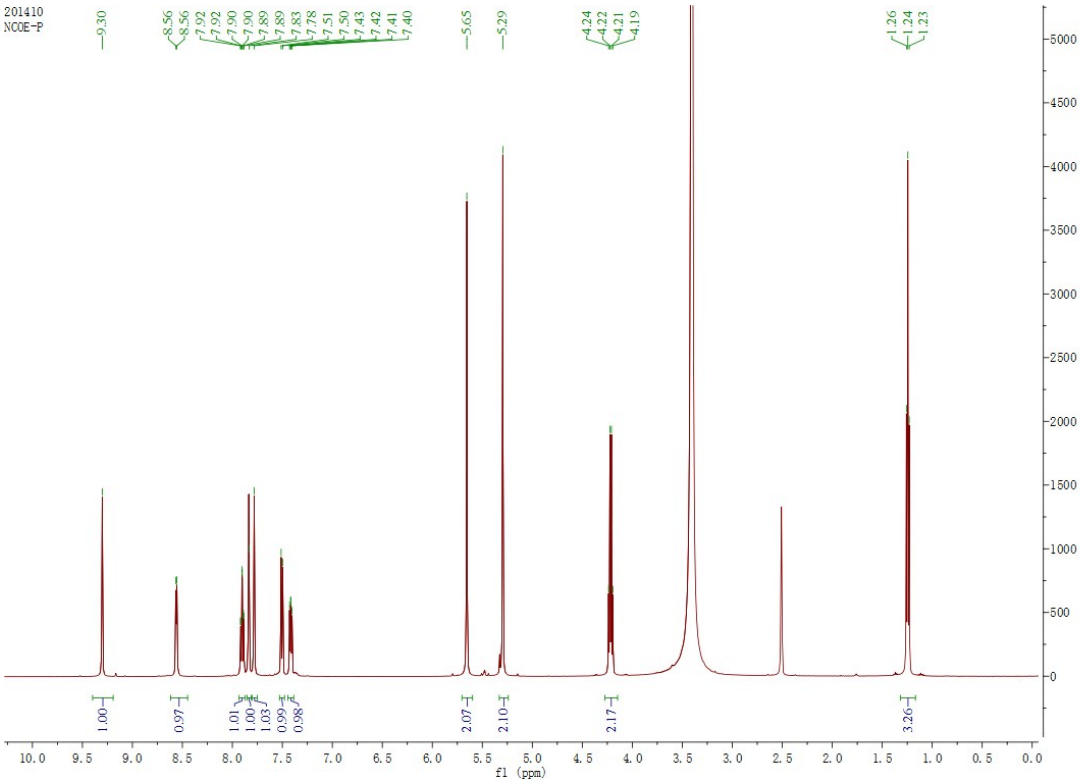

Figure S3. ^{1}H-NMR spectrum of compound **B** in DMSO-d_6.

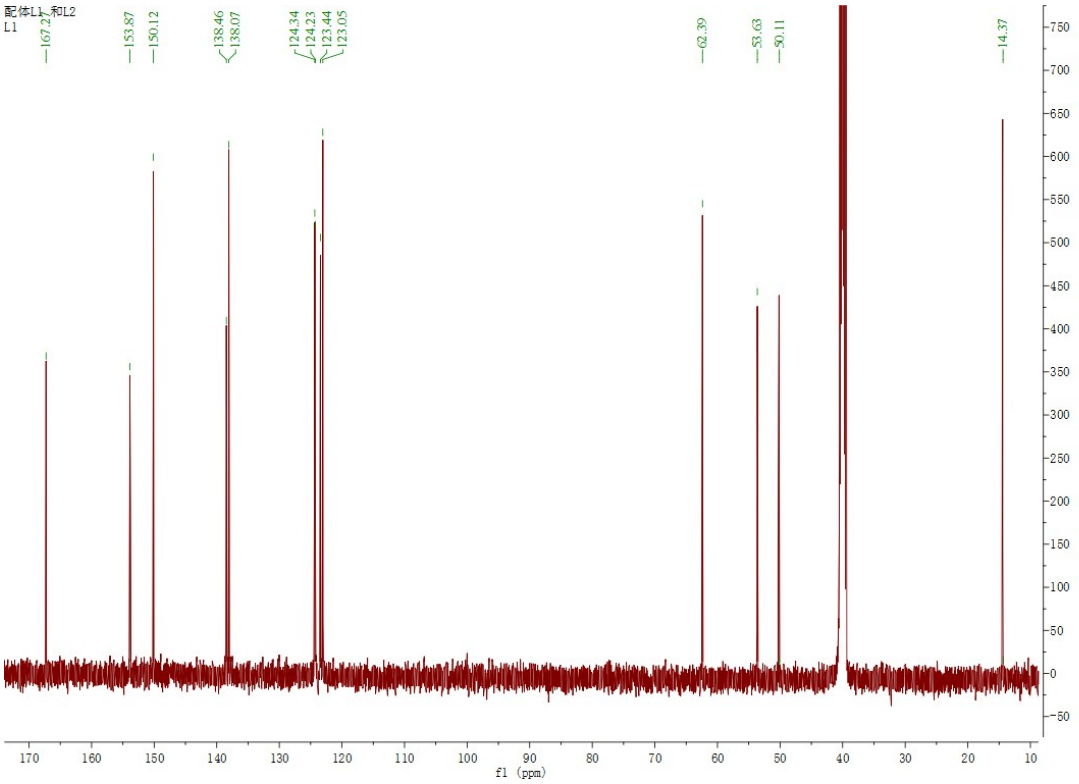

Figure S4. ^{13}C-NMR spectrum of compound **B** in DMSO-d_6**.**

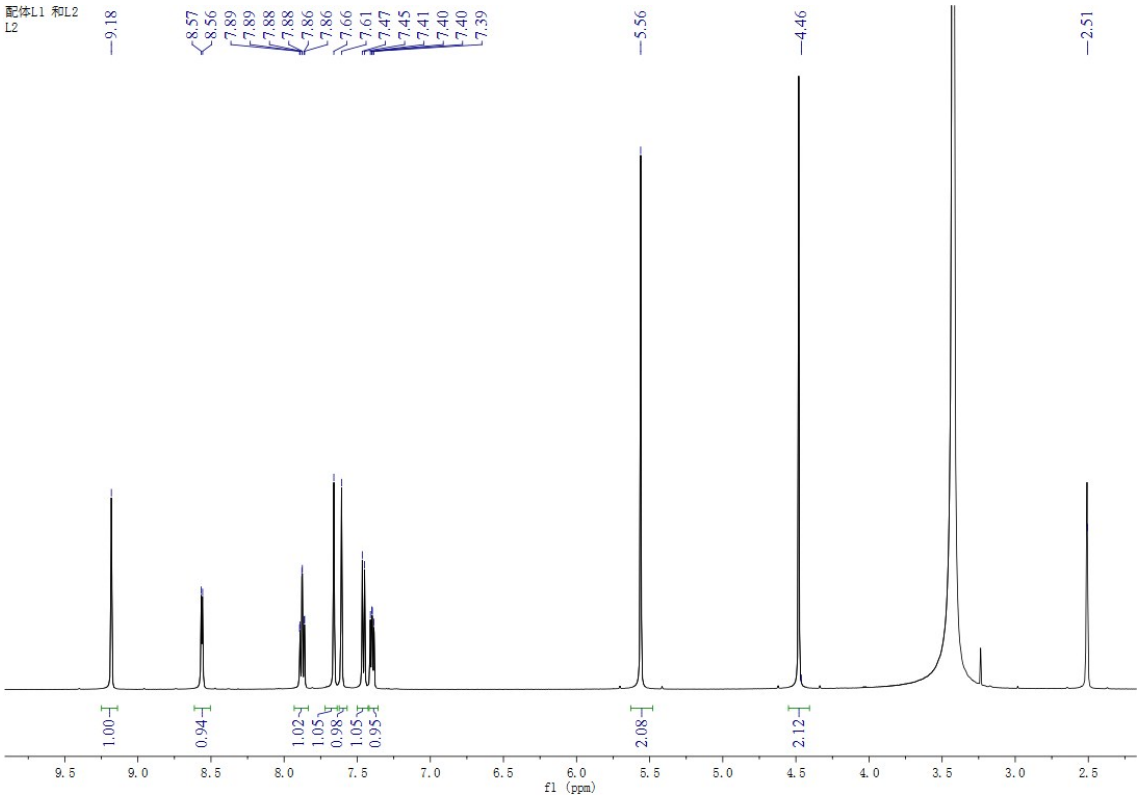

Figure S5. ^{1}H-NMR spectrum of ligand **1** in DMSO-d_6.

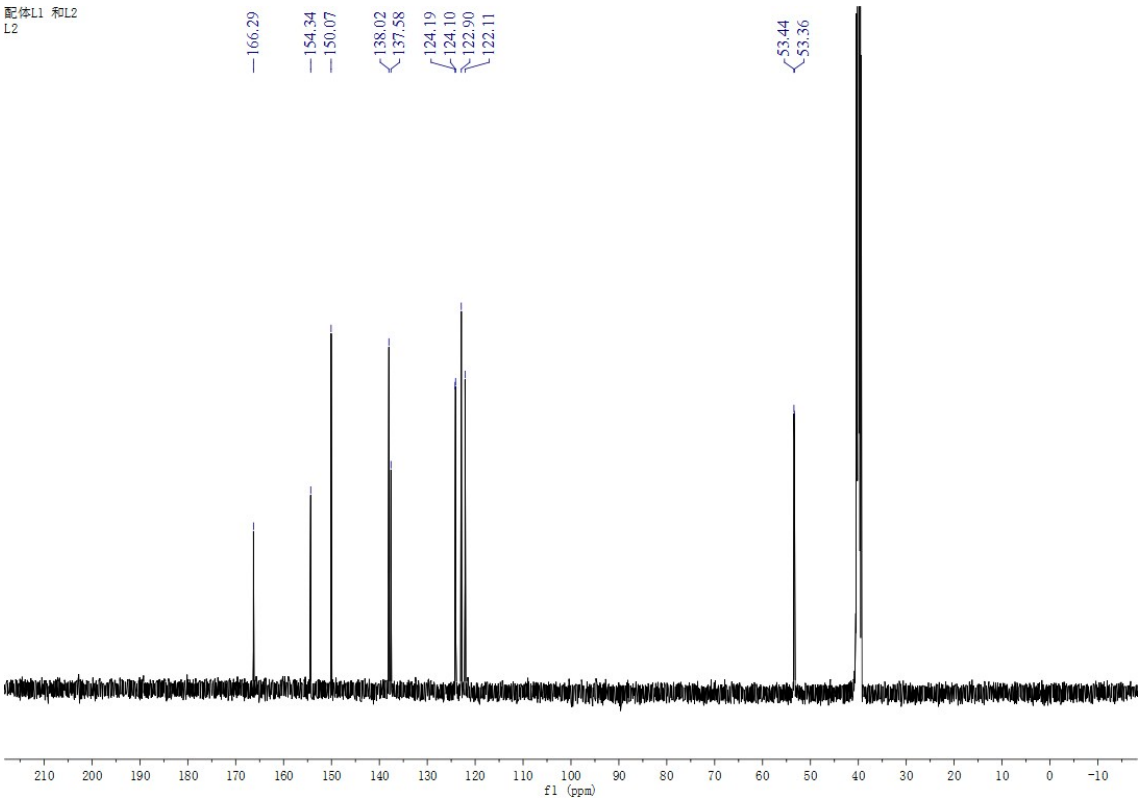

Figure S6. ^{13}C-NMR spectrum of ligand **1** in DMSO-d_6**.**

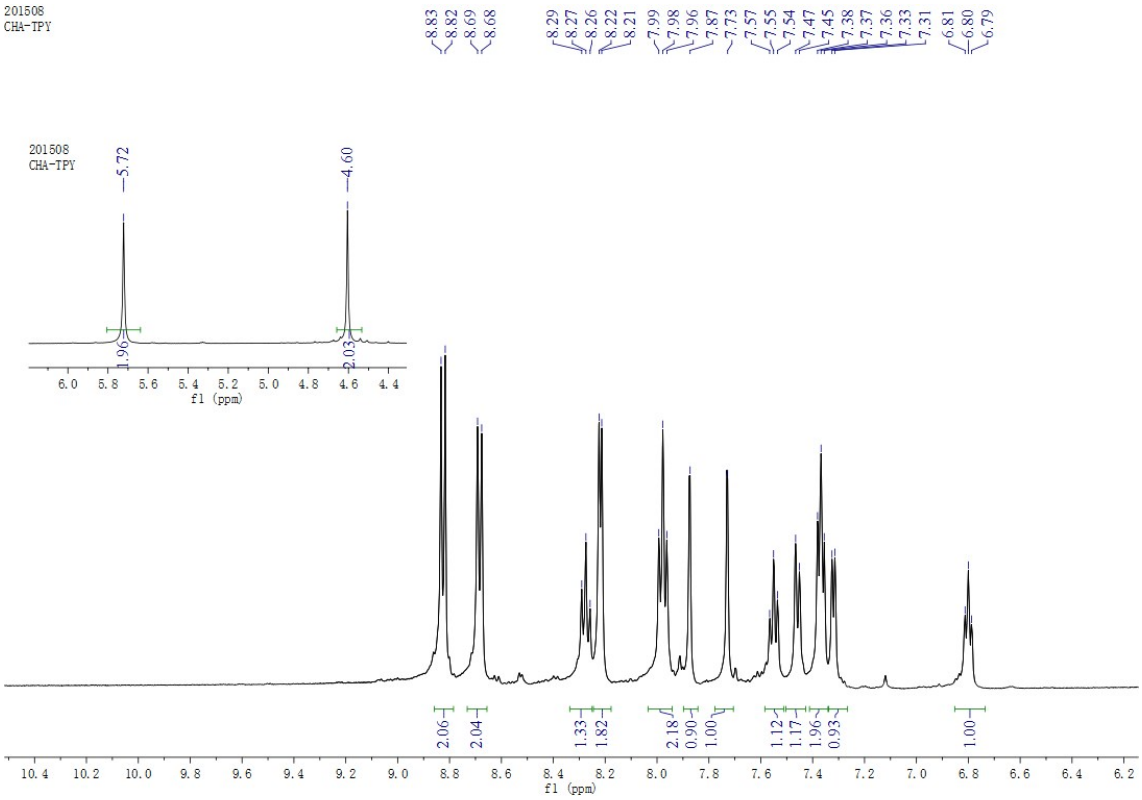

Figure S7. ^{1}H-NMR spectrum of complex **2** in DMSO-d_6.

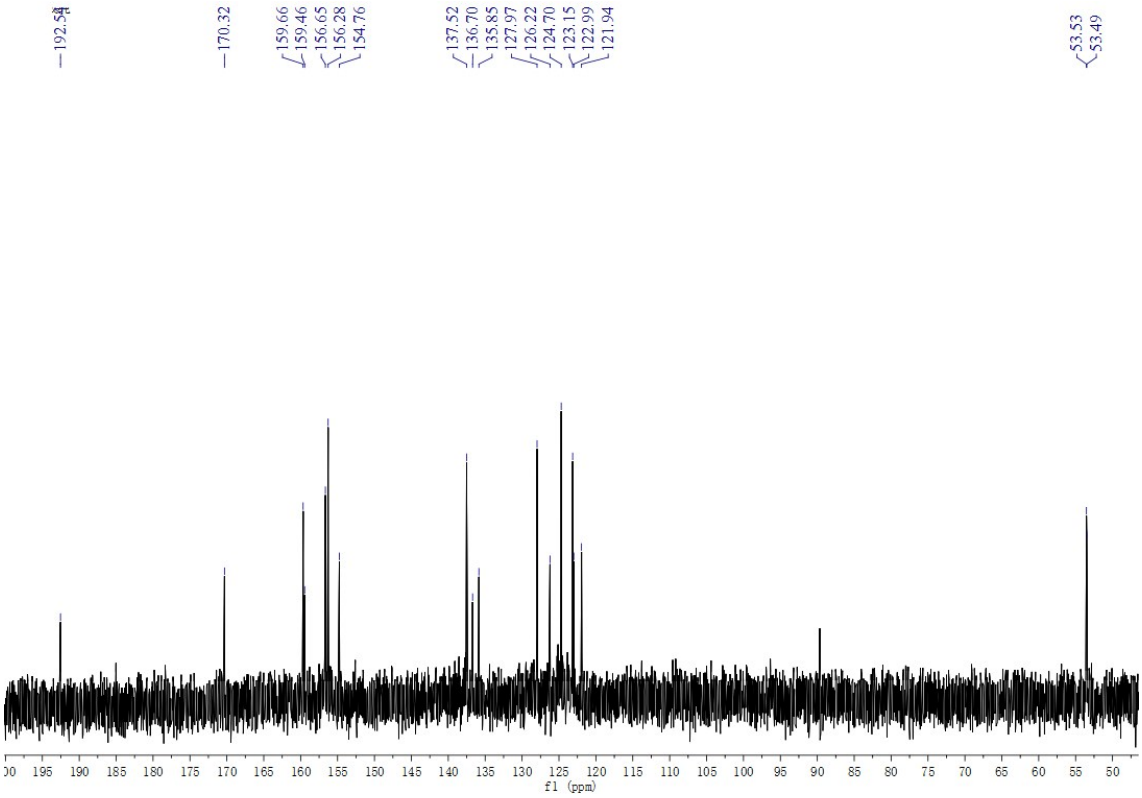

Figure S8. ^{13}C-NMR spectrum of complex **2** in DMSO-d_6.

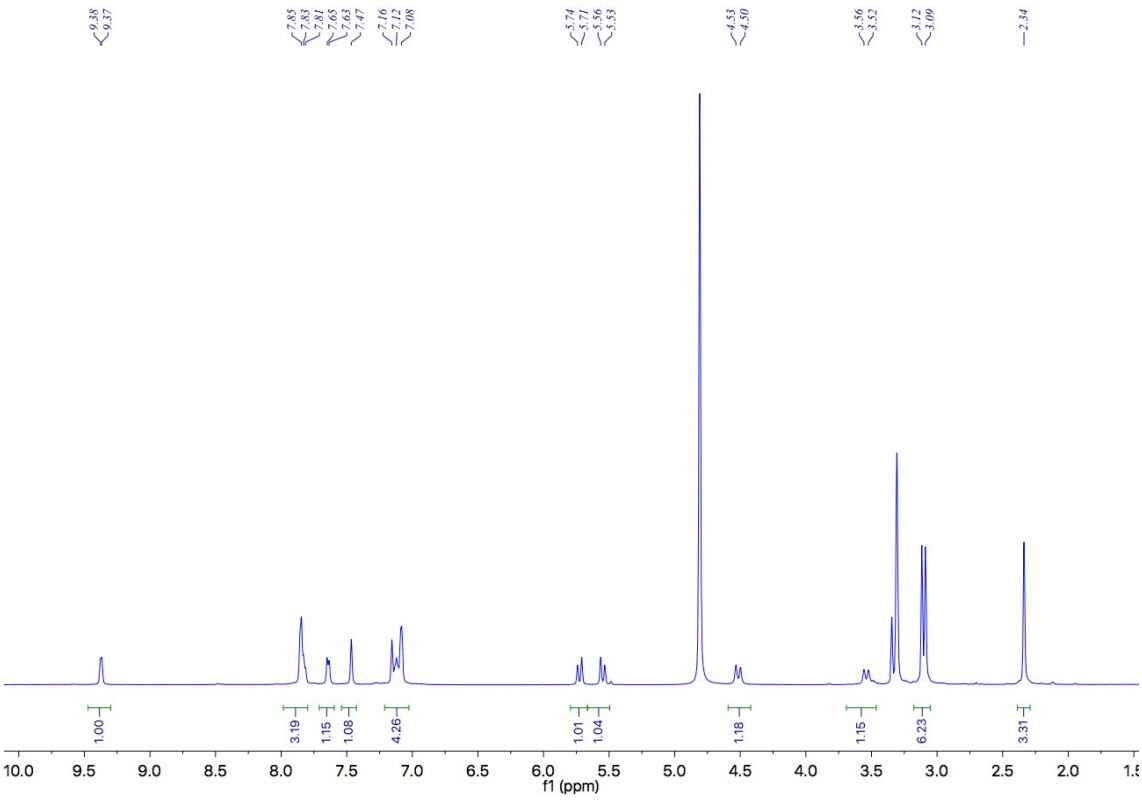

Figure S9. ^{1}H-NMR spectrum of complex **3** in CD_3OD.

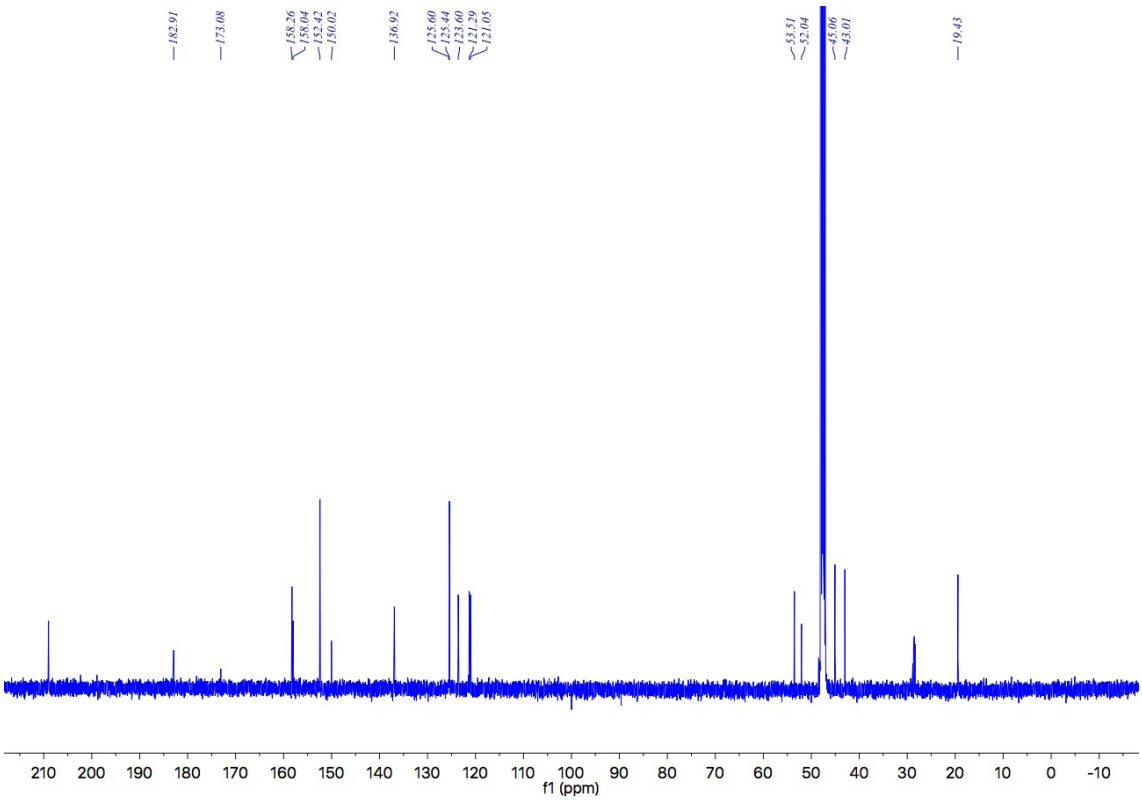

Figure S10. ^{13}C-NMR spectrum of complex **3** in CD_3OD.

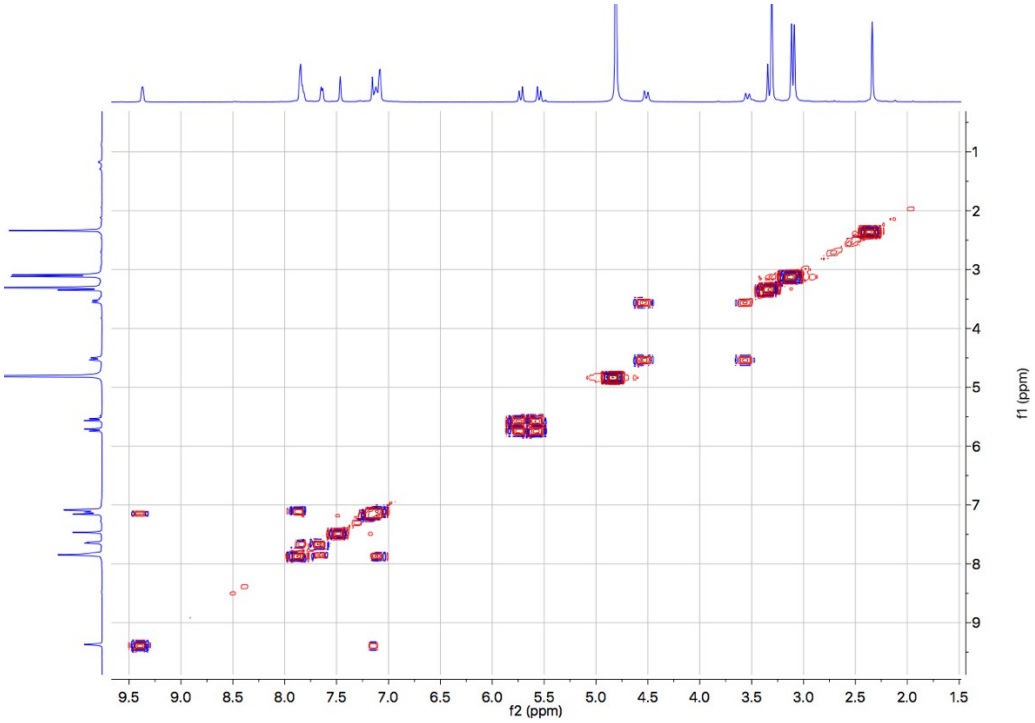

Figure S11. H-H COSY NMR spectrum of complex **3** in CD_3OD.

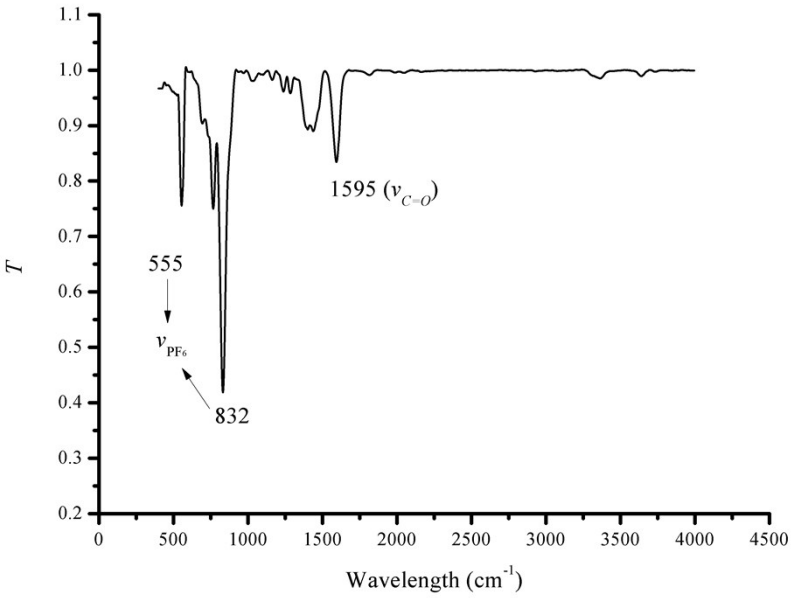

Figure S12. FT-IR spectrum of complex **2** ranging from 400 to 4000 cm^{-1} at 298 K.

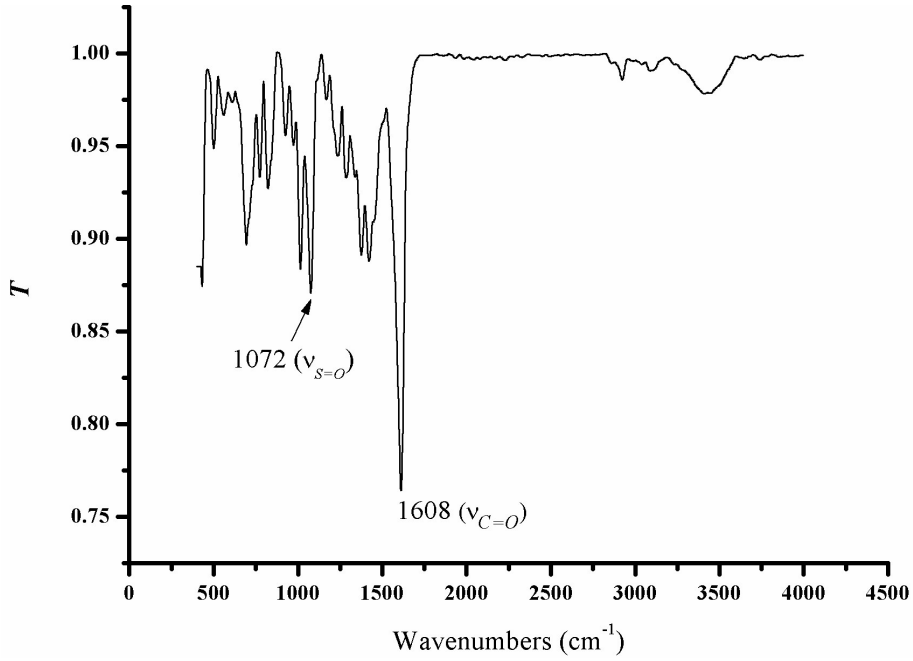

Figure S13. FT-IR spectrum of complex **3** ranging from 400 to 4000 cm^{-1} at 298 K.

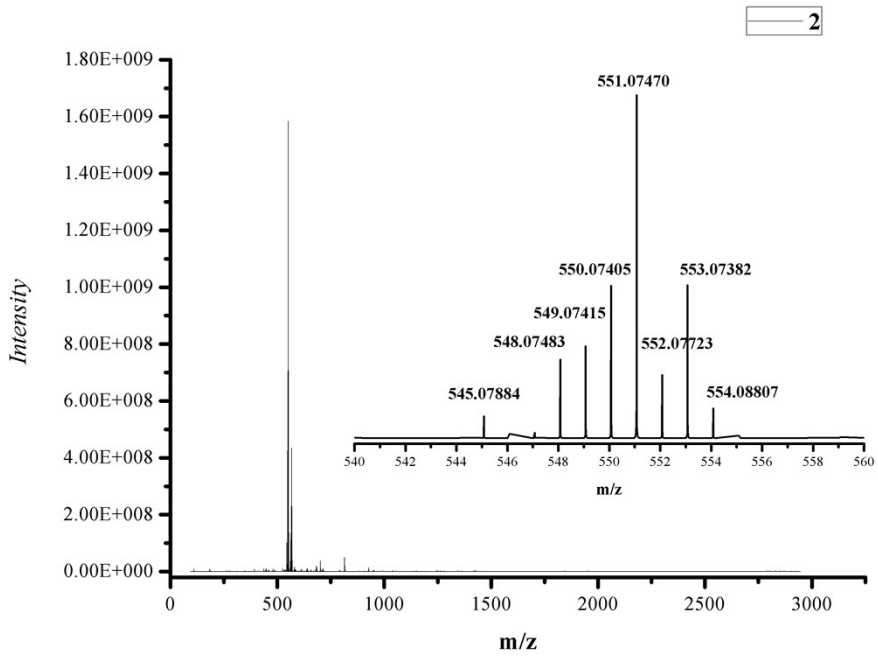

Figure S14. HR-MS (ESI) of complex **2** in positive mode with methanol as solvent.

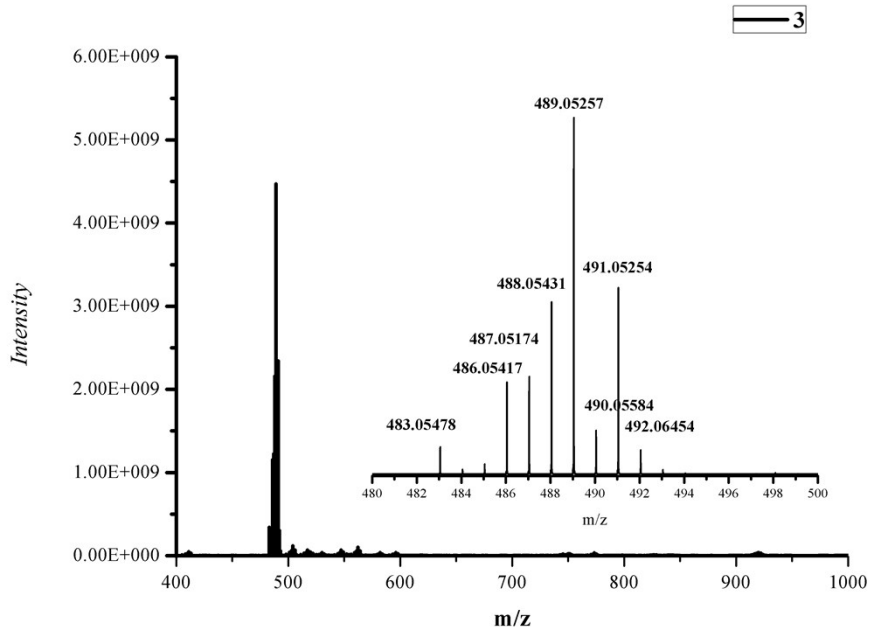

Figure S15. HR-MS (ESI) of complex **3** in positive mode with methanol as solvent.

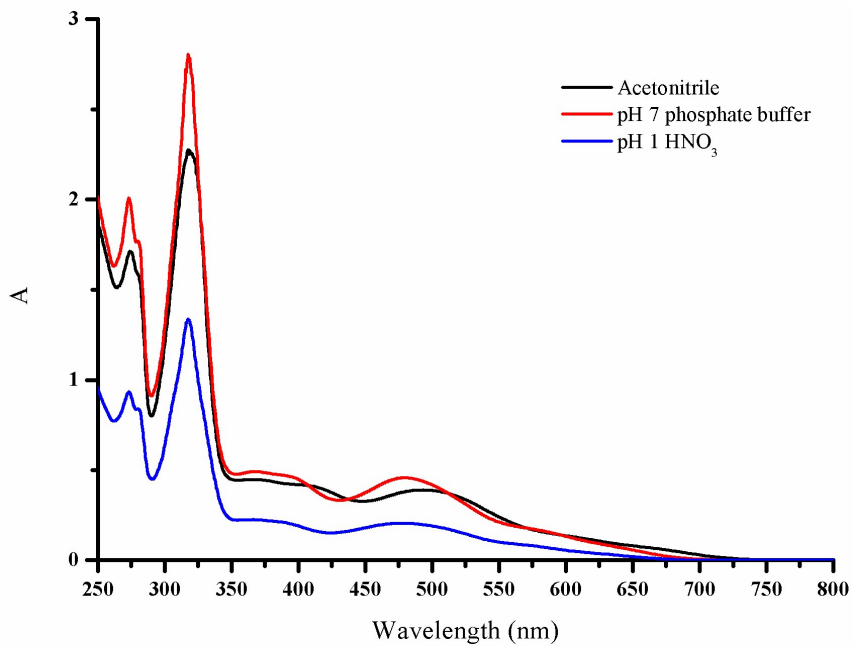

Figure S16. UV-Vis spectra of Ru complex **2** in pH 1 HNO_3 aqueous solution (blue), in pH 7 phosphate buffers (0.1 M) (red) and in acetonitrile solution (black).

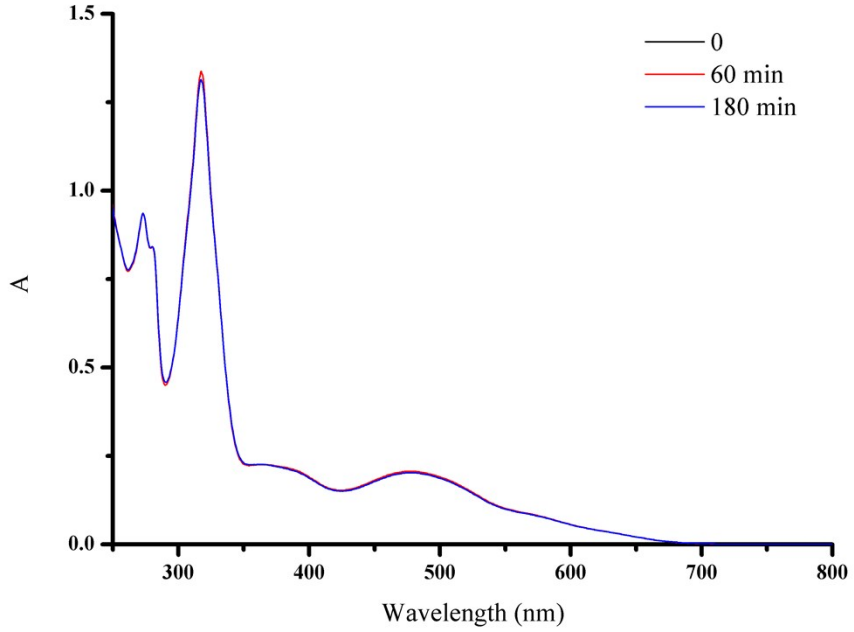

Figure S17. UV-Vis spectra of Ru complex **2** in HNO_3 aqueous solution (pH 1.0) over a 180 min period.

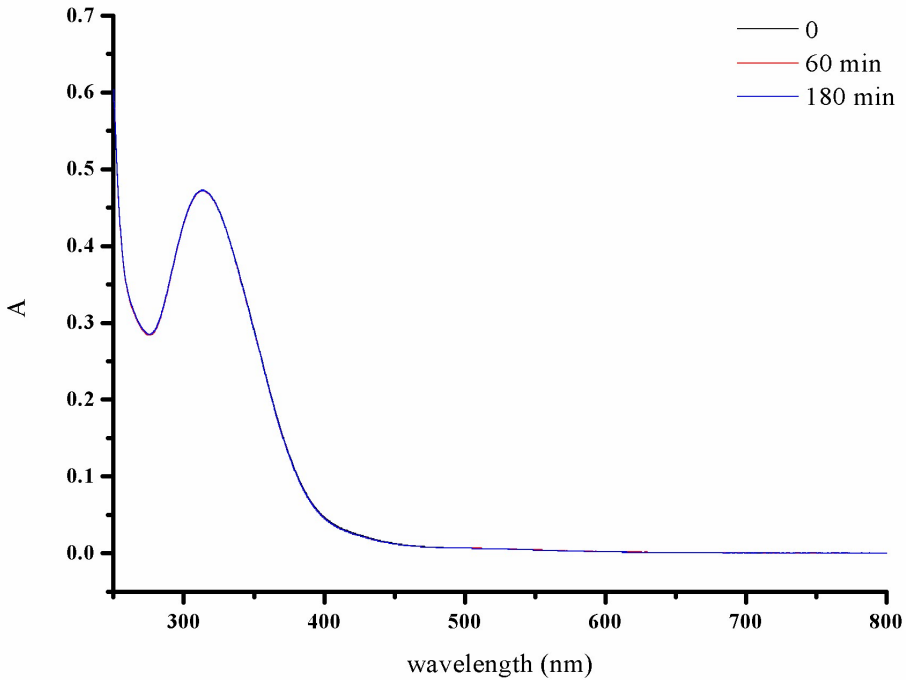

Figure S18. UV-Vis spectra of Ru complex **3** in phosphate buffer solution (pH 7, 0.1 M) over a 180 min period.

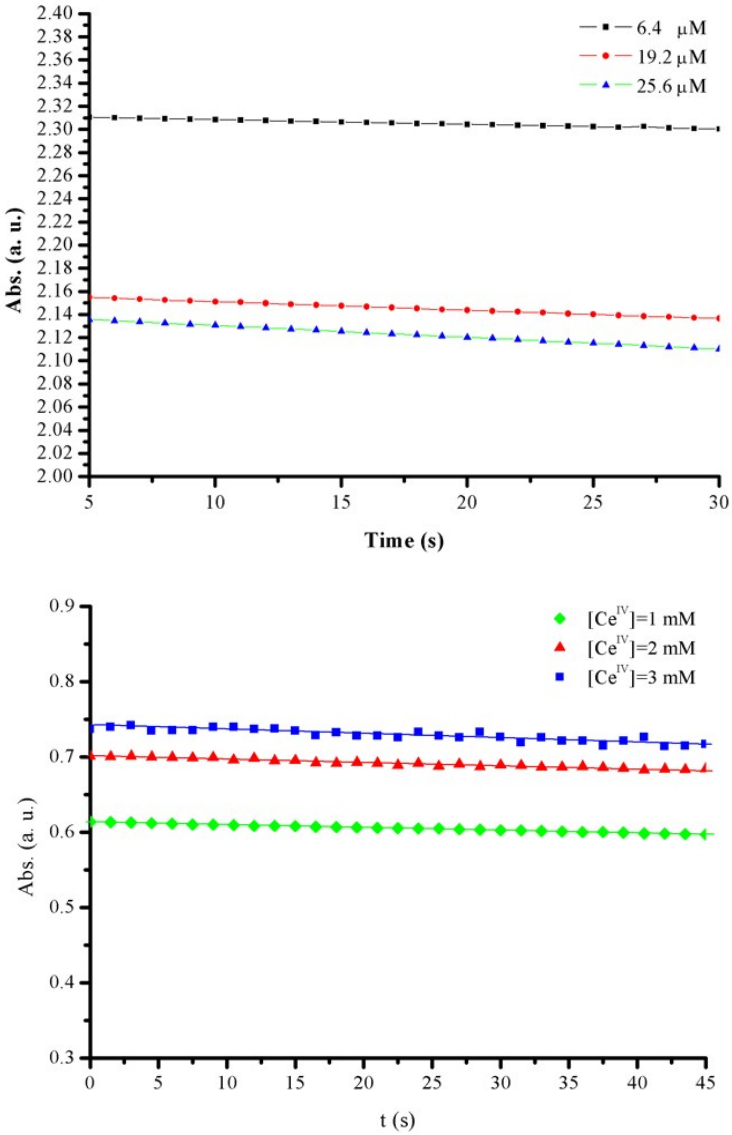

Figure S19. (Top) Absorbance changes (360 nm) at various concentration of **2**$^+$; conditions: initial [Ce^{IV}] = 3.2 mM, pH 1 HNO_3. (Bottom) Absorbance changes (360 nm) at various concentration of [Ce^{IV}] in the presence of **2**$^+$. conditions: initial [**2**] = 0.05 mM, pH 1 HNO_3.

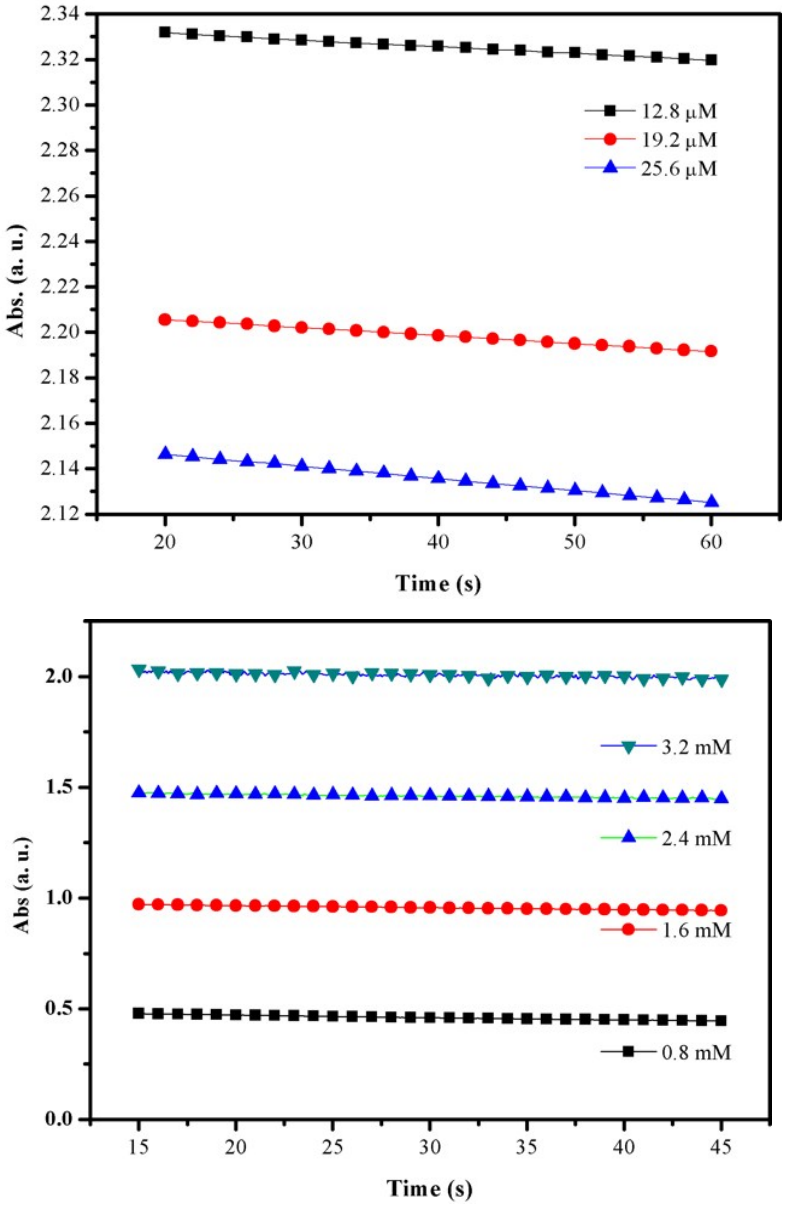

Figure S20. (Left) Absorbance changes (360 nm) at various concentration of **3**; conditions: initial [Ce^{IV}] = 3.2 mM, pH 1 HNO_3. (Right) Absorbance changes (360 nm) at various concentration of [Ce^{IV}] in the presence of **3**; conditions: initial [**3**] = 0.04 mM, pH 1 HNO_3.

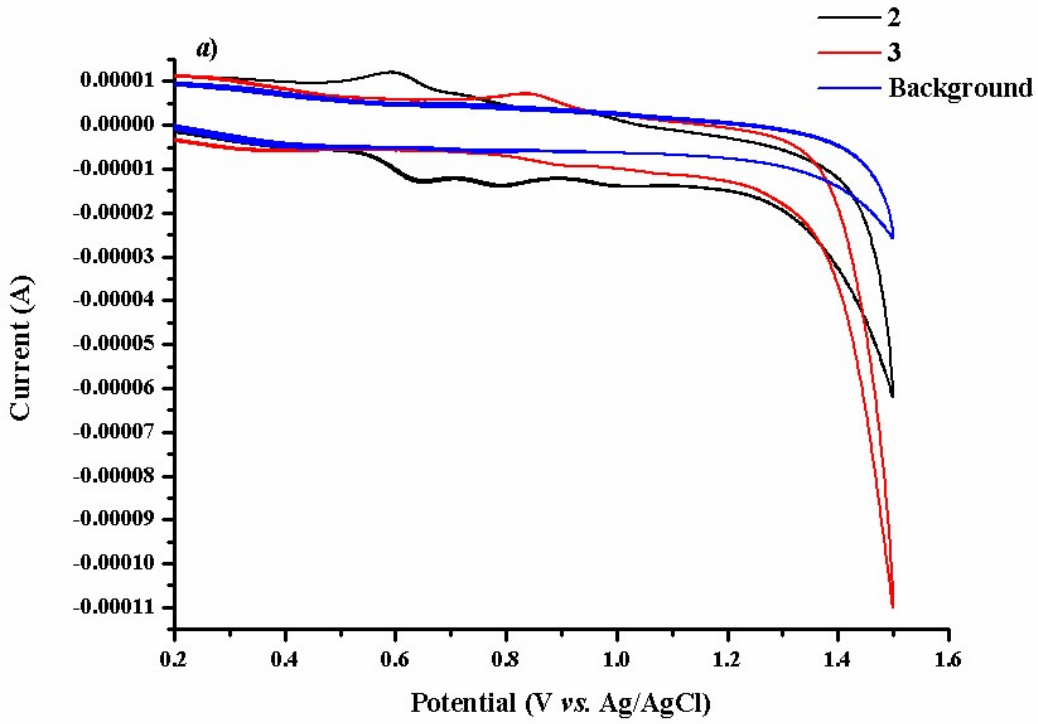
a)
2
3
Background
0.00001
0.00000
-0.00001
-0.00002
-0.00003
-0.00004
-0.00005
-0.00006
-0.00007
-0.00008
-0.00009
-0.00010
-0.00011
Current (A)
0.2
0.4
0.6
0.8
1.0
1.2
1.4
1.6
Potential (V vs. Ag/AgCl)

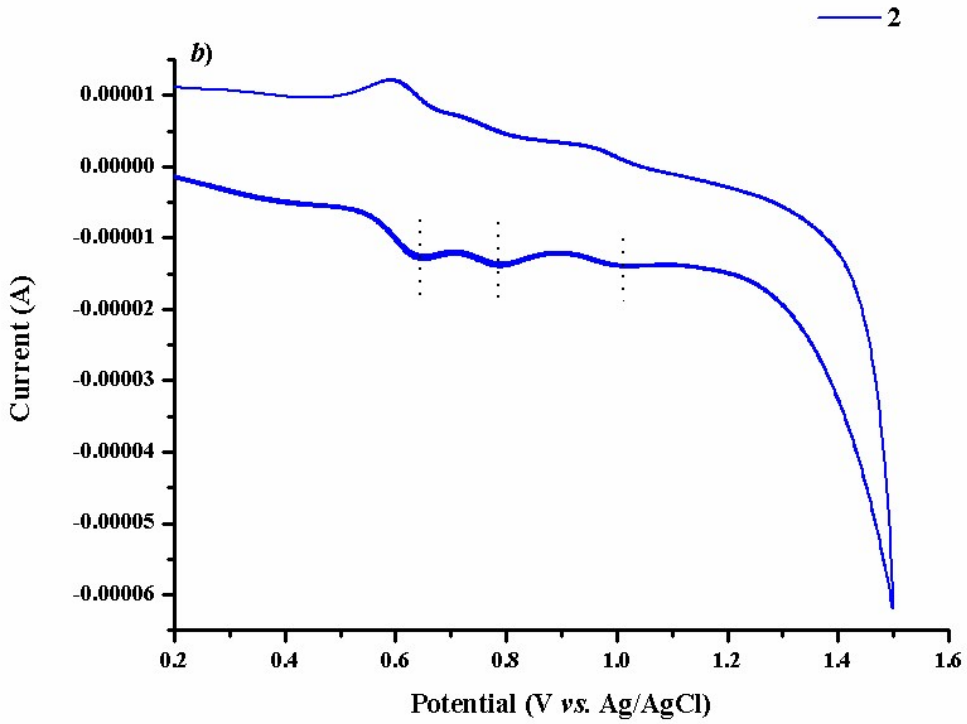
b)
2
0.00001
0.00000
-0.00001
-0.00002
-0.00003
-0.00004
-0.00005
-0.00006
Current (A)
0.2
0.4
0.6
0.8
1.0
1.2
1.4
1.6
Potential (V vs. Ag/AgCl)

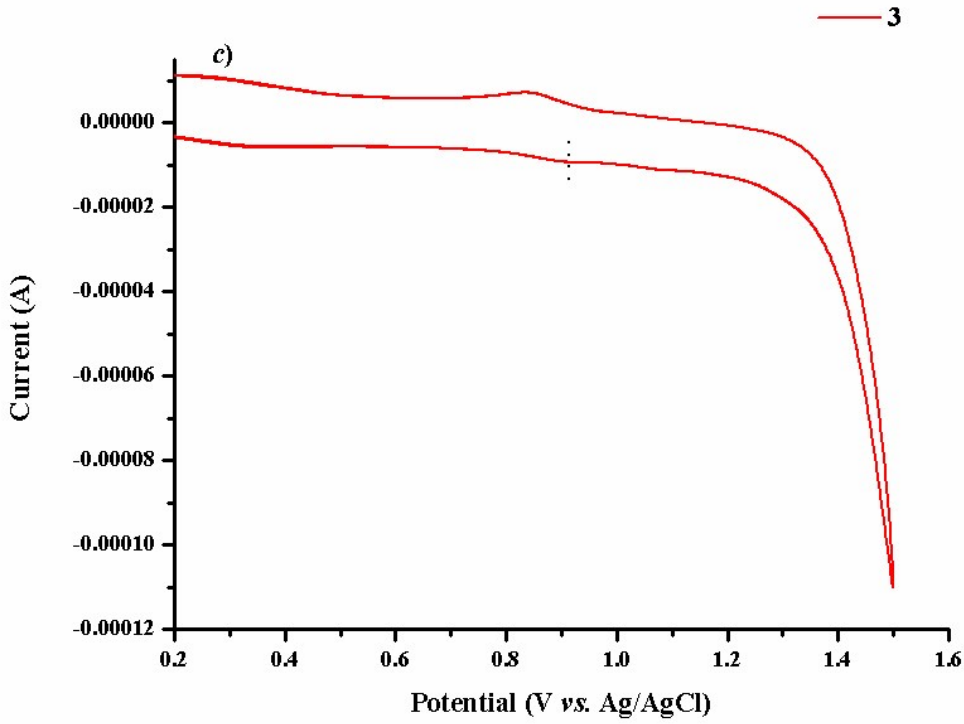

Figure S21. Cyclic voltagram of complexes (a) **2**$^+$, **3** and background; (b) **2**$^+$ and (c) **3** in pH 1 HNO_3 aqueous solution, respectively.

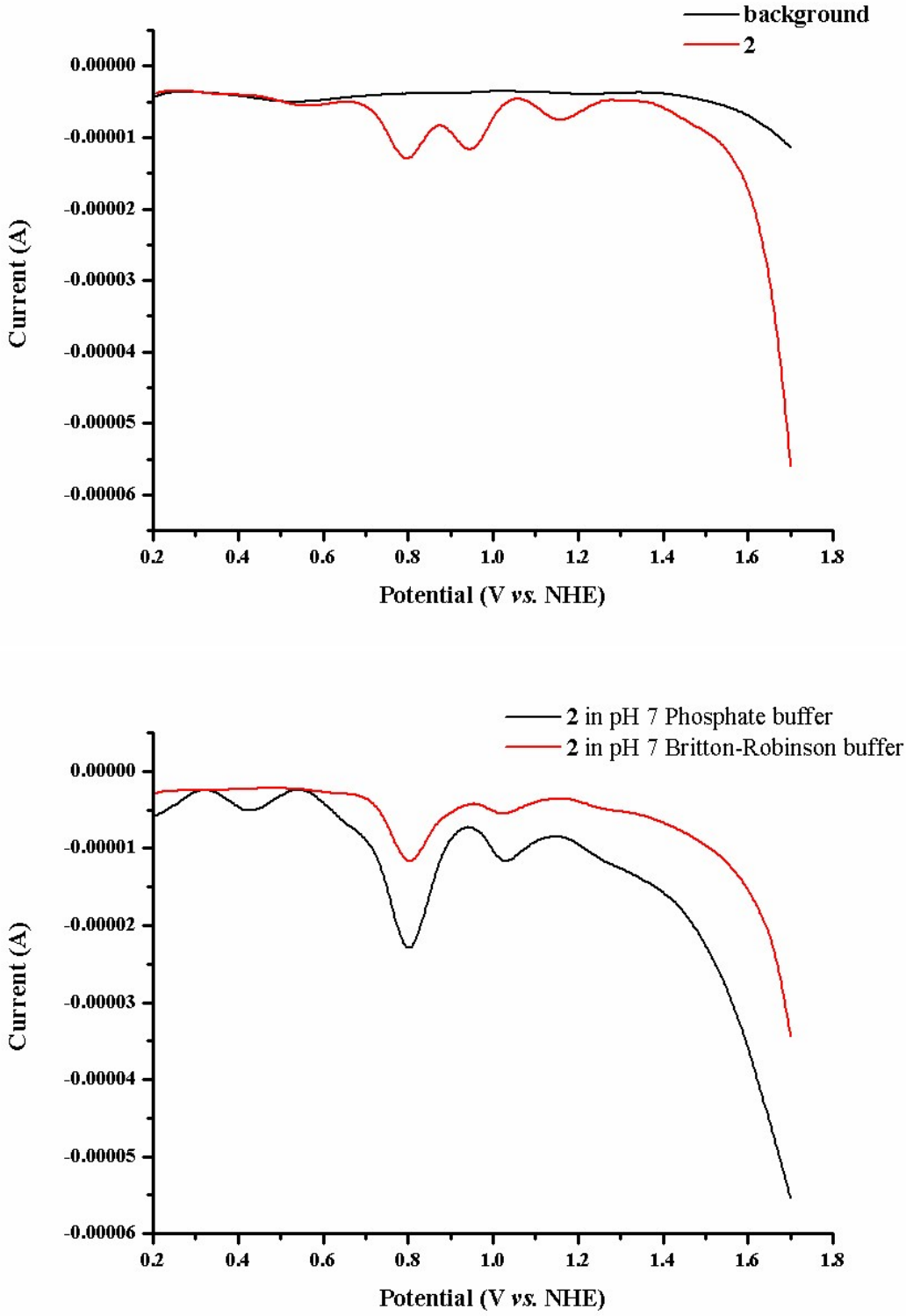

Figure S22. DPV of complex **2**$^+$ (0.1 mM) in (top) pH 1 aqueous solution (adjusted by HNO_3) and (bottom) pH 7 phosphate buffer solution and Britton-Robinson buffer (0.1 M). The broad and weak peaks appearing at less than 0.7 V *vs.* NHE are attributed to impurities in the electrolytes.

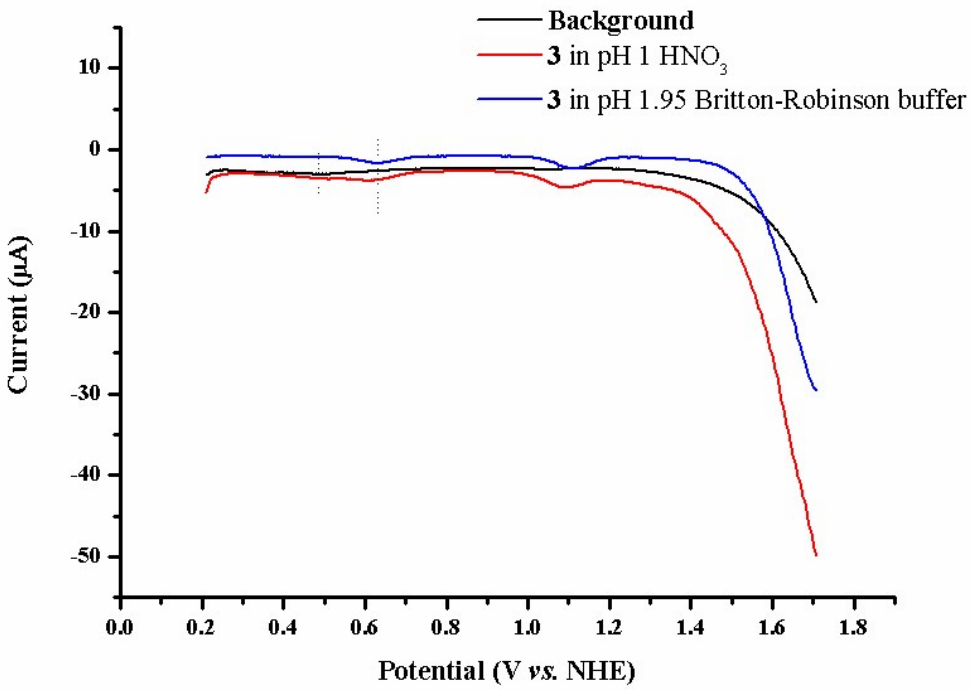

Figure S23. DPV of complex **3** (0.1 mM) in pH 1 aqueous solution (adjusted by HNO_3) and pH 1.95 Britton-Robinson buffer. Shoulder appearing at around 0.45 V is attributed to impurities in electrolytes.

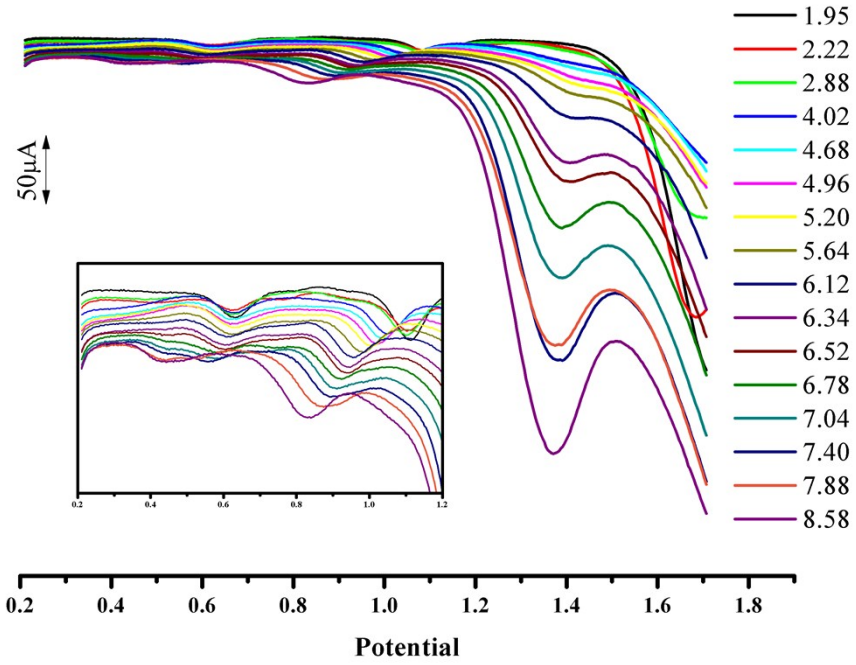

Figure S24. Differential Pulse Voltammetry (DPV) traces in the range between pH 1.5 and 9.0 for the construction of Pourbaix diagram of complex **3**. Experimental Conditions: 0.1 mM **3**, 0.1 M Britton-Robinson buffer solution. the pH of the solution was changed by addition of 0.1 mM NaOH aqueous solution. 3 mm diameter glassy carbon disk working electrode (polished between scans), Pt wire counter electrode and SSCE reference electrode. Inset: the enlarged part from 0.2 to 1.2 V *vs.* NHE.

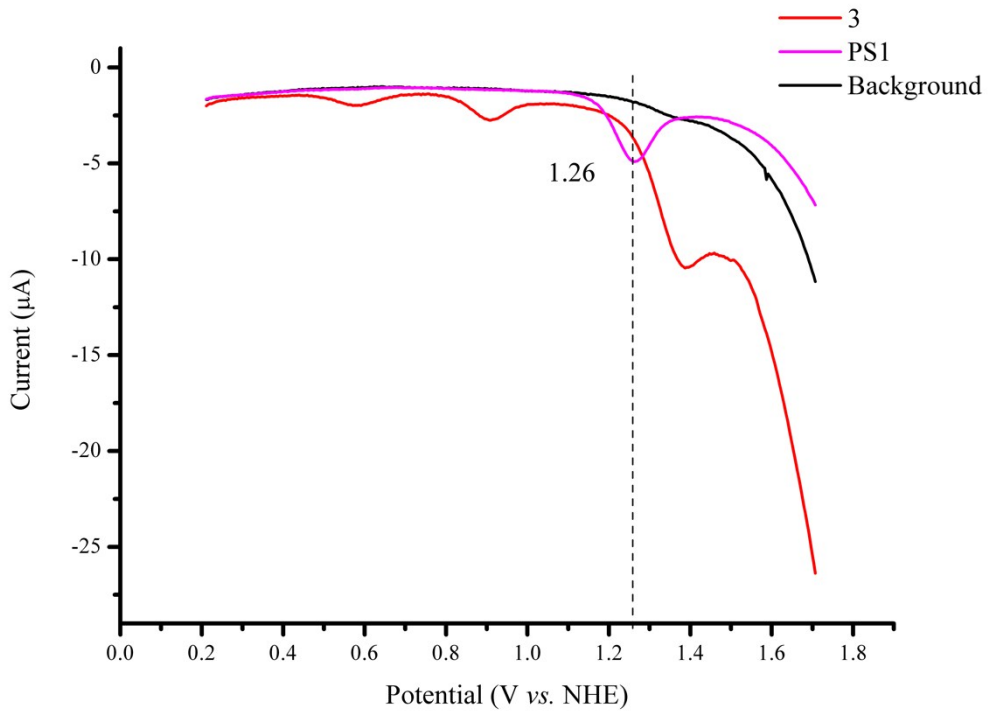

Figure S25. DPV of **3** (0.1 mM) in phosphate buffer aqueous solution (pH 7, 0.1 M), at a scan rate 100 mV/s. with **PS1** as a reference.

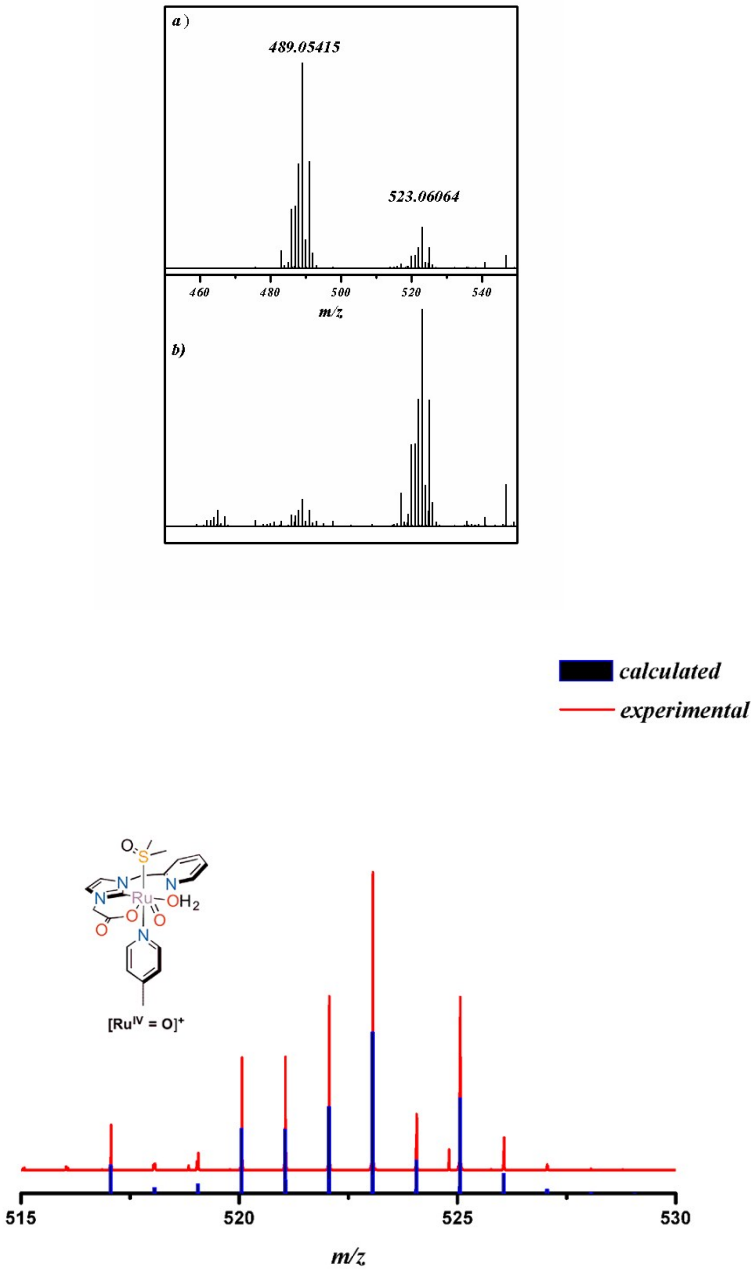

Figure S26. (Top) Detection of $[Ru^{IV} = O]^+$ derived from **3** (0.125 mM) in phosphate buffer solution (pH 7) by addition of (a) 0.5 equiv. and (b) 1.5 equiv. $NaIO_4$. (Bottom) Experimental (red) and calculated (blue) Isotope peaks of $[Ru^{IV} = O]^+$.

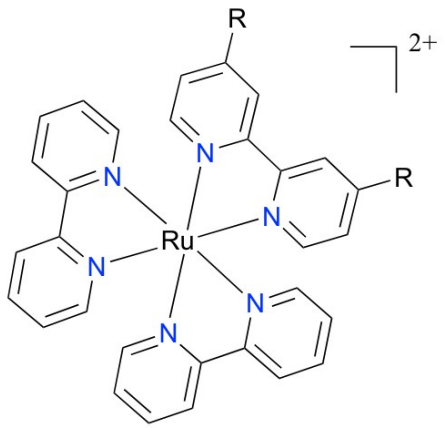

PS1: R = H

PS2: R = COOEt

Figure S27. Chemical structure of **PS1** and **PS2.**

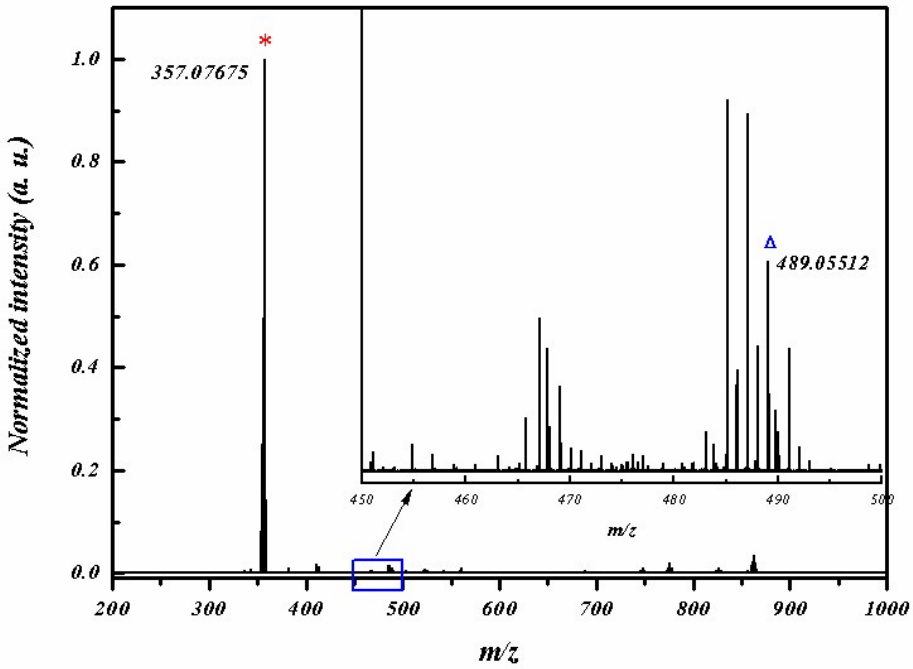

Figure S28. ESI-MS (positive ion mode) of a mixture of complex **3** (0.25 mM), **PS2** (12 equiv.) and $Na_2S_2O_8$ (800 equiv.) before illumination in pH 7 phosphate buffer. Peak marked with * is assigned to **PS2**, $[M\text{-}2Cl]^{2+}$ (calculated m/z = 357.07643). Peak marked with Δ is assigned to $[\mathbf{3}\text{-}Cl]^{+}$, (calculated m/z = 489.05345).

Table S1. Overview of different WOCs capable of initiating photo-induced water oxidation[a]

Entry	WOCs	Onset Potential (v)	TONs[b]	Ref.
1	**3**	1.21	273[c]	This work
2	**3**	1.21	33[d]	
3	**2**	1.35	10[c]	This work
4	Ru(pdc)(pic)$_3$	1.26	62[c]	S2
5	Ru(hqc)(pic)$_3$	1.05	42[c]	S3
6	Ru(hqc)(pic)$_3$	1.05	<5[d]	
7	Ru(bpc)(pic)$_3$	>1.35	NR[e]	S4
8	[Ru2(bcpPz)(pic)$_6$]$^+$	1.30	92.5[c]	S5
9	Ru$_2$Co-(H$_2$O)$_4$	1.20	16[d]	S6
10	Ru(hpbc)(pic)$_3$	1.24	200[c]	S7
11	[Ru(H$_2$bcbPa)(pic)$_6$]$^{2+}$	1.20	415[c]	S8

[a] All the experiments were carried out in neutral phosphate buffer aqueous solution; onset potential is reported *vs.* NHE; [b] TON=$n_{O2}/n_{\text{metal center}}$. [c] using **PS2**. [d] using **PS1**. [e] NR = not reported.

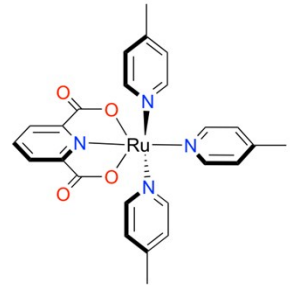

$Ru^{II}(pdc)(pic)_3$

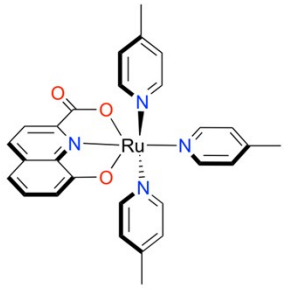

$Ru^{II}(hqc)(pic)_3$

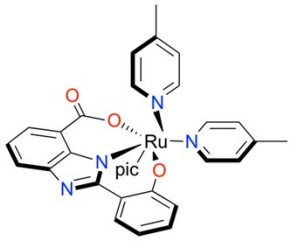

$Ru^{III}(hpbc)(pic)_3$

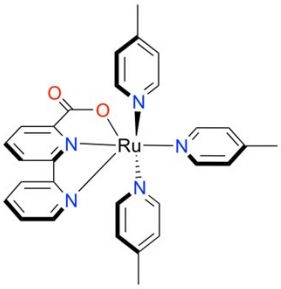

$Ru^{II}(bpc)(pic)_3$

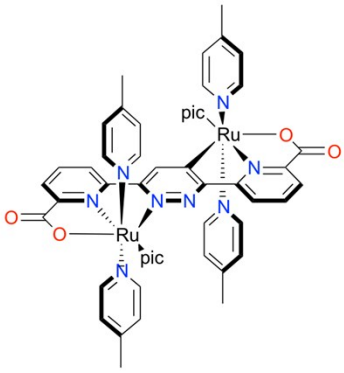

$[Ru^{II}_2(bcpPz)(pic)_6]^+$

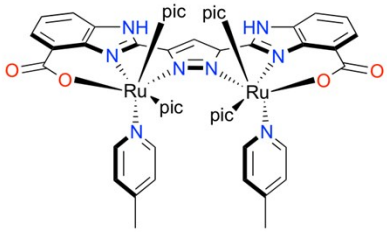

$[Ru^{II}Ru^{III}(H2bcbPa)(pic)_6]^{2+}$

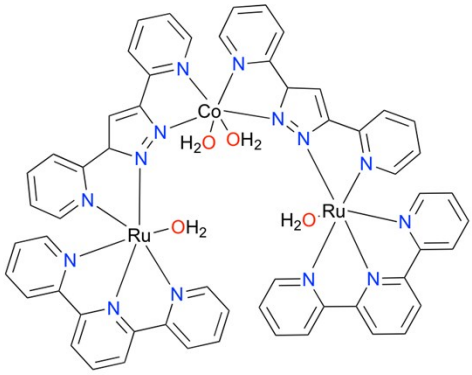

$[Ru^{II}_2Co\text{-}(H_2O)4]^{4+}$

Figure S29. Molecular structures of Ru complexes in Table S1.

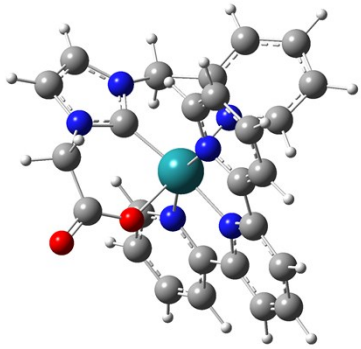

Figure S30. Calculated structures of complex **2**$^{+}$ ([Ru(NC^{NHC}O)(terpy)]$^{+}$) .

Computational details. The geometry optimizations in the present study were performed using the Gaussian 09[S9] package and the B3LYP[S10] functional. To complex **2**$^{+}$, the 6-31G(d,p) basis set was applied for the C,N, O, H elements and the SDD[S11] pseudopotential for Ru.

Table S2. Cartesian coordinates for **2**$^{+}$ ([Ru(NC^{NHC}O)(terpy)]$^{+}$).

Center Number	Atomic Number	Atomic Type	Coordinates(Angstroms)		
			X	Y	Z
1	6	0	-2.124672	-0.058255	2.225567
2	6	0	-2.583274	-0.454209	3.483932
3	6	0	-1.710425	-1.023734	4.407123
4	6	0	-0.379064	-1.182685	4.033768
5	6	0	0.009878	-0.786739	2.760574
6	7	0	-0.829031	-0.238106	1.850049
7	1	0	-2.061319	-1.32927	5.387246
8	1	0	-3.627362	-0.303512	3.737605
9	1	0	0.355149	-1.609845	4.70795
10	1	0	1.036442	-0.905544	2.439205
11	6	0	-3.087804	0.689372	1.321129
12	1	0	-4.095611	0.59113	1.728182

13	1	0	-2.832524	1.757358	1.356751
14	6	0	-4.256501	0.193448	-0.880309
15	6	0	-1.988259	0.041326	-0.793224
16	1	0	-5.255172	0.345892	-0.502208
17	6	0	-3.810323	-0.073031	-2.133459
18	1	0	-4.350034	-0.210717	-3.057159
19	7	0	-3.124092	0.251368	-0.067833
20	7	0	-2.422384	-0.164489	-2.063298
21	6	0	-1.54728	-0.505286	-3.192872
22	1	0	-2.043115	-0.190226	-4.11062
23	1	0	-1.430727	-1.595513	-3.235537
24	6	0	-0.12159	0.113696	-3.221148
25	8	0	0.525664	0.321095	-2.111367
26	8	0	0.340842	0.300835	-4.33562
27	6	0	1.748962	-2.22033	-0.137629
28	6	0	-0.421011	-3.013369	-0.490107
29	6	0	2.251806	-3.520883	-0.225487
30	6	0	0.023506	-4.327481	-0.586848
31	1	0	-1.471084	-2.764991	-0.591215
32	1	0	3.315125	-3.697747	-0.114669
33	1	0	-0.690018	-5.124035	-0.766253
34	6	0	2.50978	1.314261	0.355947
35	6	0	2.603183	-1.036927	0.10333
36	6	0	3.903457	1.386981	0.431972
37	6	0	3.999247	-1.01694	0.168618
38	1	0	4.410668	2.339715	0.524785
39	1	0	4.578771	-1.925589	0.057476
40	6	0	1.570855	2.457028	0.311959
41	6	0	-0.618467	3.159113	-0.073748
42	6	0	1.985058	3.78339	0.455128
43	6	0	-0.26386	4.498909	0.046427
44	1	0	-1.635377	2.870677	-0.311184

45	1	0	3.026133	4.006261	0.656386
46	1	0	-1.016628	5.26817	-0.084997
47	7	0	0.405189	-1.971544	-0.274776
48	7	0	1.905317	0.112427	0.241803
49	6	0	1.387196	-4.586879	-0.455533
50	1	0	1.771245	-5.598796	-0.529296
51	6	0	4.643846	0.206747	0.351449
52	1	0	5.726759	0.24452	0.401303
53	6	0	1.062934	4.817799	0.327675
54	1	0	1.377963	5.850484	0.433696
55	7	0	0.25633	2.147613	0.071796
56	44	0	-0.092811	0.066212	-0.145935

Reference:

[S1]. L. C. Pei, C. L. Lai, C. F. Chang, C. H. Hu, H. M. Lee, *Organometallics* 2005, **24**, 6169-6178.

[S2] L. Duan, Y. Xu, M. Gorlov, L. Tong, S. Andersson, L. Sun, *Chem. Eur. J.* 2010, **16**, 4659-4668.

[S3] L. Tong, Y. Wang, L. Duan, Y. Xu, X. Cheng, A. Fischer, M. r. S. Ahlquist, L. Sun, *Inorg. Chem.* 2012, **51**, 3388-3398.

[S4] L. Tong, A. K. Inge, L. Duan, L. Wang, X. Zou, L. Sun, *Inorg. Chem.* 2013, **52,** 2505-2518.

[S5] Y. Xu, L. Duan, L. Tong, B. Åkermark, L. Sun, *Chem. Commun*. 2010, **46**, 6506-6508

[S6] L. Mognon, S. Mandal, C. E. Castillo, J. Fortage, F. Molton, G. Aromí, J. Benet-Buchhlolz, M.-N. Collomb, A. Llobet, *Chem. Sci.* 2016, **7**, 3304-3312.

[S7] M. D. Kärkäs, T. Åkermark, E. V. Johnston, S. R. Karim, T. M. Laine, B. L. Lee, T. Åkermark, T. Privalov, B. Åkermark, *Angew. Chem. Int. Ed.* 2012, **51**, 11589-11593.

[S8] T. M. Laine, M. D. Kärkäs, R.-Z. Liao, T. Åkermark, B.-L. Lee, E. A. Karlsson, P. E. Siegbahn, B. Åkermark, *Chem. Commun.* 2015, **51**, 1862-1865.

[S9]. M. J. Frisch, G. W. Trucks, H. B. Schlegel, G. E. Scuseria, M. A. Robb, J. R. Cheeseman, G. Scalmani, V. Barone, B. Mennucci, G. A. Petersson, et. al. Gaussian 09, Revision B.01, Gaussian, Inc., Wallingford CT, 2009.

[S10]. A. D. Becke, *J. Chem. Phys*. 1993, **98**, 5648-5652.

[S11]. D. Andrae, U. Häuβermann, M. Dolg, H. Stoll and H. Preuβ, *Theor. Chim. Acta*. 1990, **77**, 123-141.